

INTERNATIONAL SOCIETY FOR SOIL MECHANICS AND GEOTECHNICAL ENGINEERING



This paper was downloaded from the Online Library of the International Society for Soil Mechanics and Geotechnical Engineering (ISSMGE). The library is available here:

<https://www.issmge.org/publications/online-library>

This is an open-access database that archives thousands of papers published under the Auspices of the ISSMGE and maintained by the Innovation and Development Committee of ISSMGE.

The paper was published in the proceedings of the 6th International Conference on Geotechnical and Geophysical Site Characterization and was edited by Tamás Huszák, András Mahler and Edina Koch. The conference was originally scheduled to be held in Budapest, Hungary in 2020, but due to the COVID-19 pandemic, it was held online from September 26th to September 29th 2021.

Cyclic pressuremeter tests with pore pressure measurements, application to CSR evaluation

P.G. Karagiannopoulos

Jean Lutz SA, Jurançon, NA, France, pkaragiannopoulos@jeanlutzsa.com

M. Peronne,

Jean Lutz SA, Jurançon, NA, France, mperonne@jeanlutzsa.com

Q.H. Dang, P. Reiffsteck

Univ. Gustave Eiffel, IFSTTAR, Marne-la-Vallée, IdF, France, quang-huy.dang@ifsttar.fr,
philippe.reiffsteck@ifsttar.fr

J. Benoit

University of New Hampshire, Durham, NH, USA, jean.benoit@unh.edu

ABSTRACT: This paper presents a testing program on liquefiable silt located in Brittany (France) using a new pressuremeter probe equipped with a miniature pore pressure transducer. This new type of small pore pressure transducer is attached directly onto the standard Ménard pressuremeter probe rubber membrane and then protected by the slotted tube. A series of cyclic tests showed the relationship between the resulting volume increase and the pore water pressure. These results are compared to traditional laboratory test results. An estimation of the relationship between cyclic stress ratio applied during the tests and the number of cycles to reach failure are presented and discussed in this paper.

Keywords: liquefaction, CSR; in situ; cyclic pressuremeter; pore pressures

1. Introduction

The pressuremeter test, as developed initially by Ménard in the sixties, consists in lowering a cylindrical probe covered with a rubber membrane in a prebored hole, and inflating the membrane in increments of pressure until the hole has approximately doubled in volume. The test and its procedures are well documented in the literature [1, 2, 3, 4]. Each pressure increment is held for 60 seconds for shallow depth tests and 120 seconds at greater depth (>50m).

Cyclic tests using the pressuremeter have also been used since the early introduction of the technique. These tests included one or more unloading-reloading loop making it possible to determine a cyclic deformation modulus. The values obtained are somewhere between the moduli measured in small deformations laboratory tests or with seismic wave propagation tests *in situ*, and the conventional Ménard modulus evaluated along the elastic phase of the expansion test [5, 6]. These cyclic tests are mainly intended to "erase" the initial disturbance of the borehole wall from predrilling [7, 8, 9] and provide a more elastic response of the soil. However, a single cycle of unload-reload is clearly insufficient to identify changes in soil characteristics under cyclic loading [10].

During the 1970s, the Association de Recherche en Géotechnique Marine (ARGEMA) (Association for Research in Marine Geotechnics) in France, brought together several consultants and research agencies dealing with offshore geotechnical issues and conducted a multi-site cyclic pressuremeter test program. The details of the experiments are summarized in several reports and articles in the proceedings of the

Symposium on the Pressuremeter and its Marine Applications (1982) in Paris [11, 12, 13]. Three procedures to perform the cyclic portion of the pressuremeter tests were carried out as visually defined in Figure 1:

- cyclic loading between two pressure limits p_M and p_m , higher or equal to the in situ horizontal effective stress and estimated from the limit pressure (e.g. 40 and 60%) (case a);
- variable cyclic loading between two pressure p_{Mi} and $p_m (\geq p'_0)$ (case b);
- cyclic loading between two or more variable pressure limits, the average of which is however constant, with the lower limit still greater than p'_0 (case c).

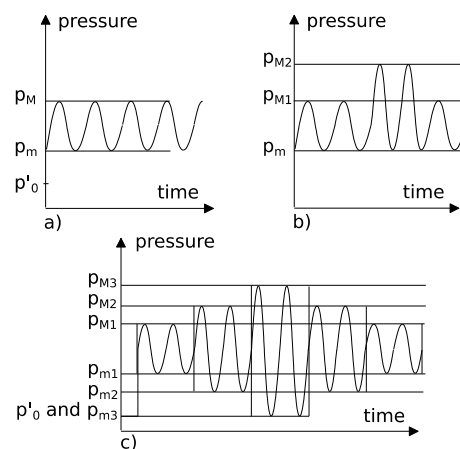


Figure 1. Cyclic pressuremeter test procedures used in the ARGEMA test program

As documented in these references, the cyclic expansion tests were carried out to assist in the design of offshore

platforms piles. The test were preferably performed using self-boring pressuremeter probes.

Others investigators such as Masuda et al. [14] have also used cyclic pressuremeter testing to soil liquefaction. Such testing required a very sophisticated and unique probe.

The objective of the work presented in this paper is to show the potential of a specially modified pre-bored pressuremeter and upgraded control system to perform high quality cyclic testing to study liquefaction in situ. The study also looked at the effect of borehole wall disturbance on the quality of the results [3, 4, 15].

1.1. Equipment

The equipment used in this research was manufactured by Jean Lutz SA (Fig. 2). It consists of a pressure volume control unit (PVCU) connected to a portable computer which operates every aspects of the test using a series of solenoid valves as well as pressure transducers and flowmeters. The volume change during probe expansion is accomplished by measuring the volume of water injected into the probe.

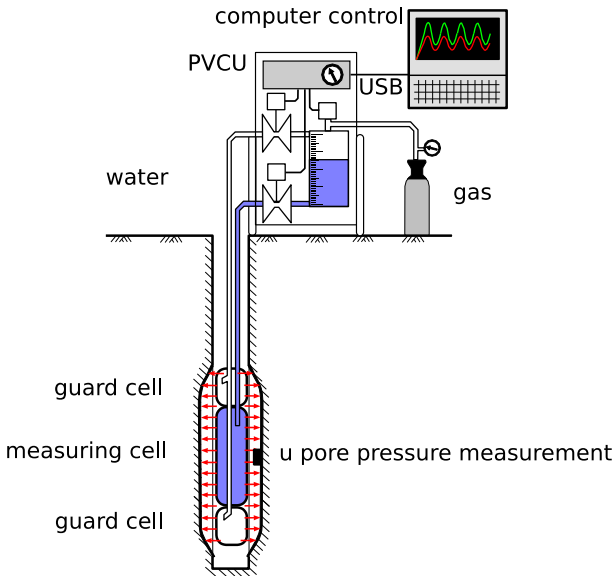


Figure 2. Schematic of the cyclic Ménard pressuremeter test

The test operations are carried out automatically either directly on the control unit or using a software program developed by Jean Lutz. The cyclic loading program allows the user to define any type of loading signal (e.g. harmonic or multiple frequencies). The data acquisition is done in real time on a datalogger.

The pressuremeter probe is a standard Ménard tri-cell probe that has been equipped with a pore pressure transducer attached to the outside of the expanding rubber membrane. The power supply to the transducer is done via a thin wire embedded in a groove in the membrane.

1.2. Test Method

For the testing campaigns presented hereafter only one loading program was used which consisted in cyclically loading between two pressure limits p_M and p_m (Fig. 3).

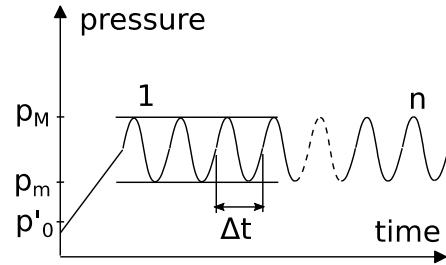


Figure 3. Cyclic portion of the pressuremeter test

The tests were carried out in pressure-controlled mode with a cyclic frequency based on soil type in an attempt to remain drained using a predefined stress level. The cycles had a frequency varying from 0.01 to 0.05 Hz and a number of cycles equal to 50.

The initial pressure p_m used to start the cyclic stage of the test is kept greater than the horizontal effective stress p'_0 while the maximum pressure p_M is selected to obtain a specific stress ratio as defined by Dupla and Canou [10]. The pressure p'_0 was estimated from previous Ménard type expansion test results using the method proposed by Briaud using the minimum curvature point as the probe recontacts the borehole wall [16, 17].

1.3. Data Analysis

Using the results from the cyclic tests, the Cyclic Stress Ratio (CSR), conventionally defined for the triaxial test as the ratio of the maximum cyclic shear stress δq over twice the consolidation stress, σ'_c (shown in Eq. 1) was used as the basis for a similar CSR for the pressuremeter:

$$CSR_{TX} = \frac{\delta q}{2 \cdot \sigma'_c} \quad (1)$$

In the triaxial test, the failure is generally defined as either when the test reaches liquefaction ($\Delta u = \sigma'_{3c}$), or at a double amplitude axial deformation of 5% reached in 20 cycles [15].

For the pressuremeter test, it is proposed to define the Cyclic Stress Ratio similarly as in the laboratory. It is the ratio of the simple amplitude δp over twice the effective earth pressure at-rest stress, p'_0 , as shown in Eq. (2):

$$CSR_{PMT} = \frac{\delta p}{2 \cdot p'_{mean}} = \frac{p_M - p_m}{4 \cdot (p_M + p_m)} \quad (2)$$

As presented on Fig. 4., tests are carried out at different pressure amplitudes Δp , and the CSR evolution curves are plotted against the number of N cycles. In Figure 4, N_L is the number of cycles to liquefaction, ε_r is the radial strain and r_u is the pore pressure ratio. These curves can then be used to predict the behavior of structures under seismic or cyclic loading. Unlike for the laboratory experiments such as the triaxial test or the

simple shear test, for *in situ* tests it is not possible to change or modify the soil density but the tests are carried out at the existing in place density.

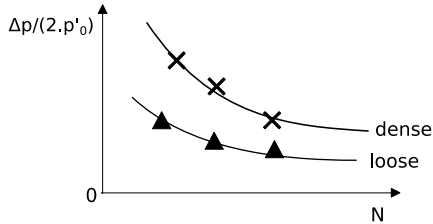
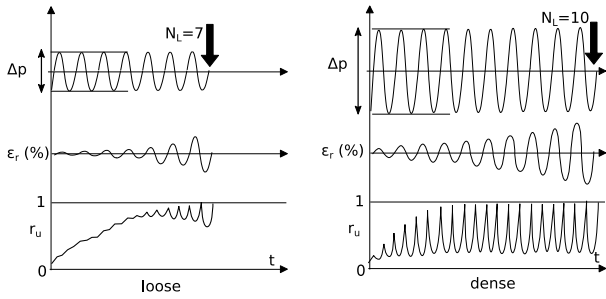


Figure 4. Cyclic behavior and CSR concept

To obtain the radial strain ε_r , it requires transforming the measured volume change during the pressuremeter expansion into a volumetric strain (Eq. 3).

$$\varepsilon_V = \frac{\Delta V}{V_0} = \frac{V - V_0}{V_0} \quad (3)$$

where: V = measured cavity volume during the test
 V_0 = initial cavity volume

The volumetric strain, ε_V is converted into radial strain ε_r , using elastic theory as shown in Eq. (4):

$$\varepsilon_V = (1 + \varepsilon_r)^2 - 1 \quad (4)$$

Failure during a pressuremeter test is defined in a similar way to the triaxial test whereas the envelope of volume (for drained conditions) versus number of cycle is determined and a power law is fitted to the accumulation curve (accumulated volume versus number of cycles). A value of $\varepsilon_V = 50\%$ or $\varepsilon_r = 21\%$ has been defined based on previous projects to fit with laboratory results. If the 50% of volumetric strain is not reached during the test (limited to 50 cycles) the number of cycles to failure is extrapolated using the power law.

2. Testing Program

2.1. Saint-Benoît-des-Ondes site

The results of a series of cyclic pressuremeter tests performed below the Duchess Anne embankment dyke close to the Mont Saint Michel (France) are presented in this section.



Figure 5. Location map of Saint-Benoît-des-Ondes

The Duchess Anne dike, built between 1020 and 1040, extends from the tip of Château Richeux (south of Cancale), in the west, to the small massif of Saint-Broladre, to the east (see map Fig.5). The dyke separates the marshland from the adjoining sea. The study focused on a 17 km linear section, the management of which is ensured by a local owners association.

The dike of the Duchess Anne was constructed taking advantage of ancient coastal ridges at this location to protect the Dol marshes from high tidal ranges (15 m tidal range in the bay). The thickness of Quaternary sediments is between 15 and 20 m below the dike and these are essentially made up of pitch (granulometric class of lutites) and fine sands. Given the proximity to the sea and being within the tidal reach, these materials are fully saturated. The marine sands are well-graded.

Fig. 6 presents the cone penetration (CPT) profiles obtained on site under the embankment and close to the Ménard pressuremeter tests (MPM) and cyclic pressuremeter tests (PMT) boreholes. Depth of watertable was 2 m during the tests.

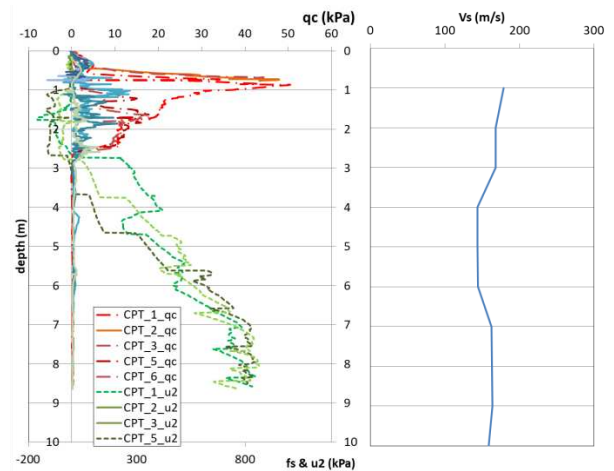


Figure 6. CPT and Vs profile at Saint-Benoît-des-Ondes

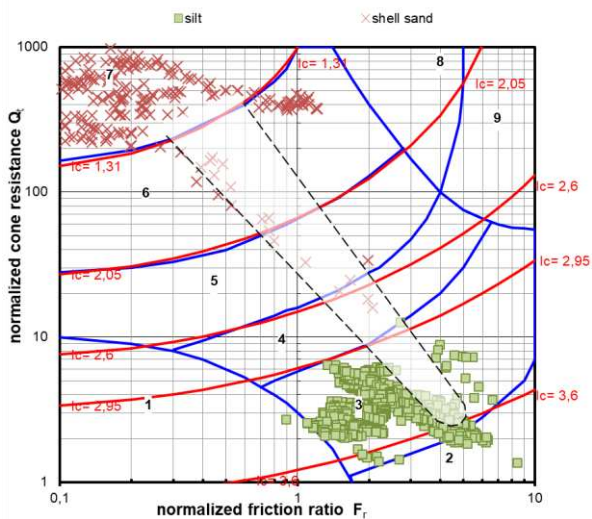


Figure 7. CPT soil behavior type chart

The results of the piezocone profiles are plotted on the soil behavior index chart of Robertson (2009) [19] on Figure 7 and suggests that the upper (red crosses) layer behaves as a coarse soil (shell sand) overlying a fine silty or somewhat cohesive soil (green squares).

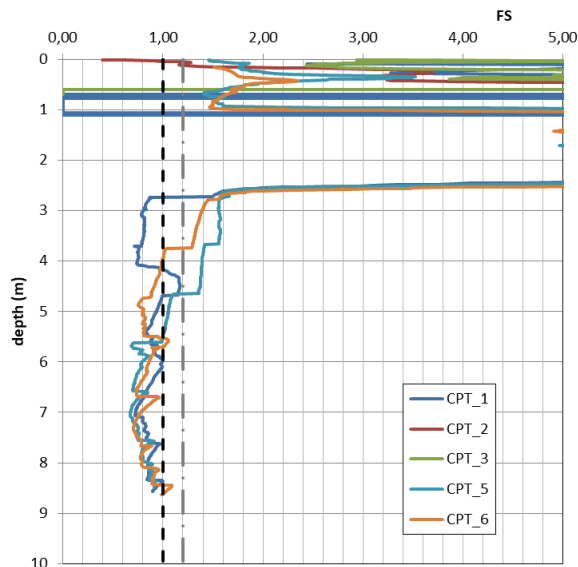


Figure 8. Liquefaction safety coefficient derived from CPT results according to NCEER

Based on the CPT results, the liquefaction threshold proposed by Youd and Idriss [20] appears to occur below 3m depth (Fig. 8).

At the Duchess Anne dyke, three separate cyclic pressuremeter test campaigns have been recently performed: 2016, 2018 and 2019. The analysis of the first set of data obtained during the 2016 campaign showed the need for improvement to achieve the same reliability than in laboratory testing. Changes were made for the 2018 testing, including a first attempt at pore pressure measurements. Figures 9 and 10 show the results using two different membrane protection systems.

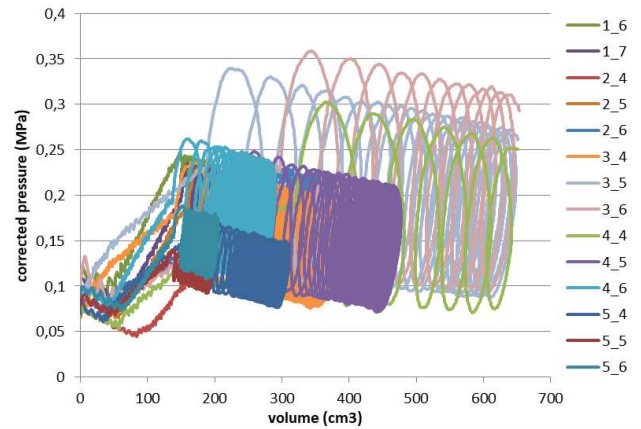


Figure 9. 2016 Test campaign - Evolution of pressure with corrected control for canvas cover

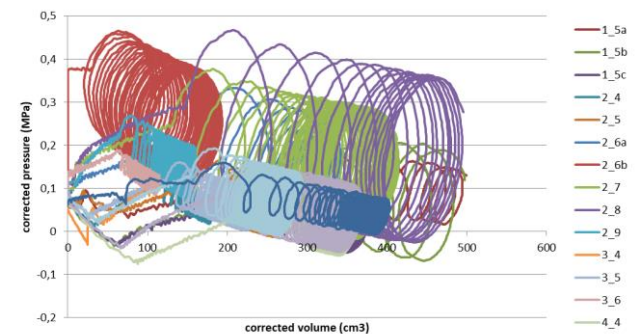


Figure 10. 2018 Test campaign - Evolution of pressure with corrected control for slotted tube

During these two campaigns, the cyclic loading was imposed between two fixed pressure set at the surface on the test control device. However, once corrected for membrane stiffness, these limits were significantly diminished at probe level. This can be observed in Figures 9 and 10 as the corrected pressure decreases as the volume increases. To avoid this discrepancy the software was later modified to take into account the pressure loss due to the membrane resistance, in real time. Once the correction is applied, the pressure at probe level stays almost perfectly between the initially defined limits which was not the case for the first two test campaigns in 2016 and 2018.

Figure 11 shows the results from 2019 obtained with the new pressure control approach for both membrane cover systems (i.e. reinforced membrane cover and membrane with slotted tube). The pressure control using the membrane-slotted tube correction appears very efficient even if some slight increase or decrease of the mean pressure is observed. This small variation is attributed to a zero offset from the initial probe volume V_0 .

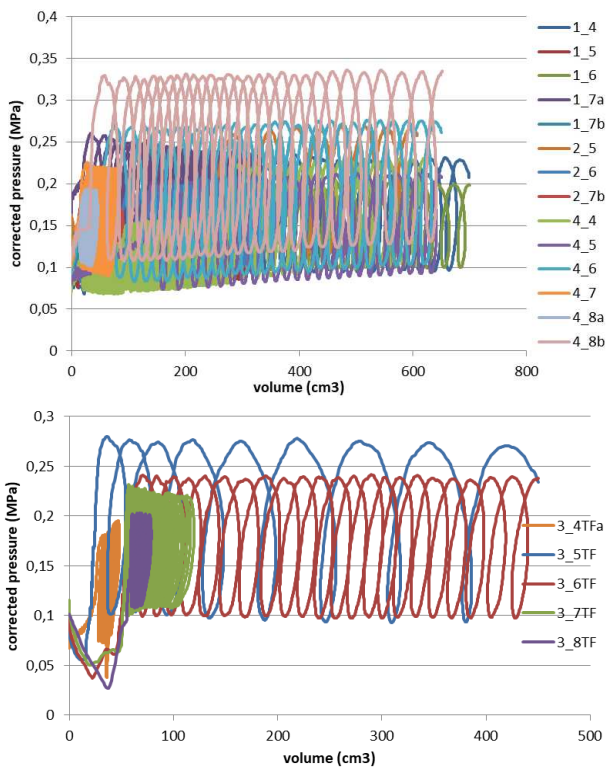


Figure 11. 2019 test campaign - Evolution of pressure with corrected pressure control for both type of probe (top: rubber membrane only and bottom: rubber membrane with slotted tube)

On Fig. 9 to 11 the influence of pressure amplitudes on the volume accumulation is clearly visible and corresponds to the behaviour previously observed by Dupla et Canou [10]. A greater hysteresis is observed in these *in situ* tests comparatively to lab tests due to the nature of the soil (wider particle size distribution), different from Hostun sand, the reference soil used in calibration chamber, as well as the pressure loss in the 25 m length of tubing in the field.

Some of the results from 2019 are shown in Fig. 12 in terms of volumetric strain versus time. As can be shown, the strain accumulates more rapidly as the amplitude of pressure increases.

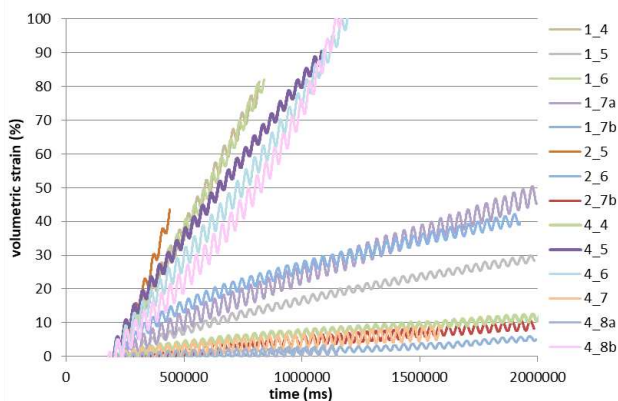


Figure 12. Volumetric strain as a function of pressure cycles (second number is depth in meters)

Fig. 13 shows the accumulation curve for the pressuremeter test 4_5 (rubber membrane only) i.e. the envelope curve, formed of the maximum volumetric strain observed during each cycle which represents the irreversible or permanent strain. To determine the

number of cycles at 50% volumetric strain a power law is fit on the accumulation curve.

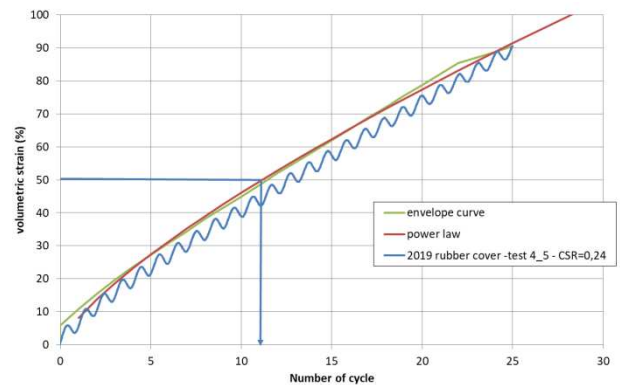


Figure 13. Definition of the accumulation curve

Fig. 14. presents the number of cycles corresponding to the conventional failure at 50 % volumetric strain according to the CSR applied to all tests of all 3 campaigns.

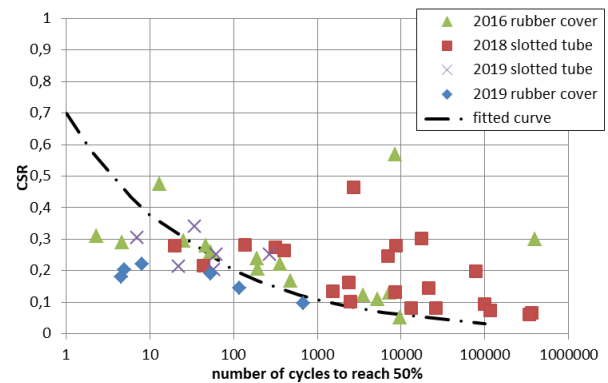


Figure 14. CSR evolution for different cover types

Fig. 14 shows that the points obtained during the three campaigns are close together and as anticipated, the difference appears to be for the highest number of cycles, i.e. for a higher volume and thus a higher influence of the pressure loss. Data from the 2018 campaign obtained using the old control approach and slotted tube are more scattered than the corrected data of the 2019 campaign using a slotted tube. Due to the decrease of the two pressure limits (upper and lower) during the first two campaigns, the actual CSR increases but the mean pressure decreases significantly during the test.

2.1.1. The evolution of pore pressure

During the last test campaign, measurement of pore pressure during the cyclic loading have been performed at mid-height of the probe as shown on Figs. 2 and 15.

This newly developed simple and robust transducer can be fixed on the standard pressuremeter probe directly on the membrane in the rubber membrane version or when using the slotted tube over the membrane.



Figure 15. Pore pressure transducer attached to the flexible membrane cover

Fig. 16. show the evolution of pore water pressure measured directly on the probe during the tests. The quality of the signal is a good indication that the transducer was working as intended. The increase in pore pressure follows the increase in the pressure cycle amplitudes.

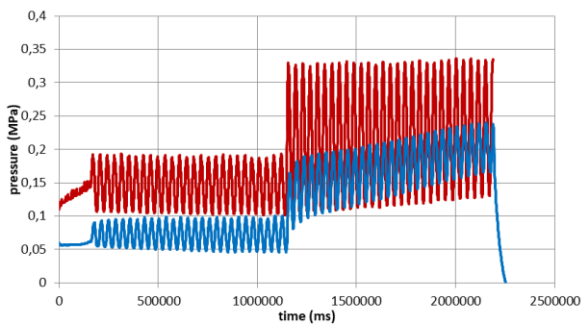


Figure 16. Example of pore pressure measurement during Saint-Benoît-des-Ondes test campaign (membrane cover, 8 m depth)

As an initial approach, a comparison of an *in situ* pore pressure ratio similar to r_u (Eq. 5) derived in the triaxial test has been made and is shown on Fig. 17. p is considered as the mean accumulation pressure.

$$r_u = \frac{u}{p} \quad (5)$$

When r_u reaches a value close to 1 the soil resistance drops dramatically as shown in Fig. 17.

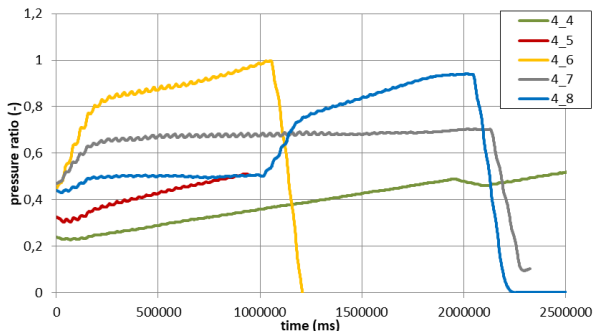


Figure 17. *in situ* r_u ratio evolution during cycling

This study is ongoing and further comparisons will be made with other *in situ* and laboratory tests.

3. Conclusions

In this paper a new ground investigation procedure to evaluate the liquefaction potential based on cyclic pressuremeter testing has been presented. The interpretation of results can be performed similarly to what is done in laboratory triaxial testing. The results suggest that a CSR curve can be proposed without the need for sampling and laboratory testing on disturbed or reconstituted samples, especially in cohesionless soils.

Once the appropriate membrane loss corrections were applied to the pressure control system, the proper test procedures lead to measurements of pore pressures which showed a progression in agreement with the volumetric strain measurements from the accumulated unload-reload cycles. The addition of pore pressure measurements offers new potential insight on the influence of fines content on pore pressure development in soils in their existing *in situ* state.

Acknowledgement

The authors thank the national project ARSCOP, the ANR project ISOLATE (grant ANR-17-CE22-0009) and the Ministry of Ecological and Solidarity Transition for funding this research project as well as their colleagues R. Benot, G. Desanneaux from CEREMA for assisting in this project.

References

- [1] Ménard L. Influence of the intensity and increment history of the stresses on the settlement of a soil of foundation, 5th ICSMFE Paris, 1961 (1)42:249-253
- [2] LCPC, Essai pressiométrique normal, (Standard pressuremeter test operating method) MS-IS-2, Eds Dunod, Paris, 1971, 50 pages (in French)
- [3] Ménard L. Règles relatives à l'exécution des essais pressiométriques, (Interpretation and application of pressuremeter tests results,) Sols Soils, 1976, 27 : 7-20 (in French)
- [4] CEN, Geotechnical investigation and testing. Field testing. Ménard pressuremeter test, EN ISO 22476-4, 2004, pp. 43.
- [5] Ménard L. Phase de déchargement des essais pressiométriques, Etude théorique et applications, (unloading phase of pressuremeter test, Theoretical study and application) Circulaire 1960, 3 pages (in French)
- [6] Borel S., Reiffsteck Ph., Caractérisation de la déformabilité des sols au moyen d'essais en place. Characterization of soil deformability using *in situ* testing (in French) LCPC Paris, 2006, pp. 132.
- [7] Hoopes O., Hughes J, In Situ Lateral Stress Measurement in Glaciolacustrine Seattle Clay Using the Pressuremeter, J. Geotech. Geoenviron. Eng., 2014, 140(5): 04013054
- [8] Combarieu O., Canépa Y., The unload-reload pressuremeter test, BLPC, 2001, 233 : 37-65
- [9] AFNOR, Reconnaissance et essais, Essai pressiométrique Ménard – partie 2, Essai avec cycle, (ground investigation and testing, Ménard pressuremeter test – part 2 test with one cycle) NF P94-110-2, 1999, pp. 43. (in French)
- [10] Dupla, J.C., Canou J. Cyclic pressuremeter loading and liquefaction properties of sands, Soils and Foundations, 2003, Vol. 43(2), 17-31
- [11] Jézéquel J.F., Le Méhauté A., Cyclic tests with self-boring pressuremeter, symposium on the pressuremeter and its marine applications, 1982, pp. 221-233.
- [12] Puech A., Bruy F., Ma E., Calcul de la capacité axiale des pieux de fondations marines à partir du pressiomètre autoforeur, (computation of axial bearing capacity of offshore foundations, based on self-boring pressuremeter) Symposium sur la pressiométrie et ses applications en mer, Paris, Éditions Technip, 1982, pp. 373-388. (in French)

- [13] Le Méhauté A., Jézéquel J.F., Essais cycliques au pressiomètre autoforeur, Cyclic tests with self-boring pressuremeter (in French) Rapports des LPC, FAER 1-05-09-22, 1980, 29 pages
- [14] Masuda, K., Nagatoh, R., Tsukamoto, Y., Ishihara, K., Use of cyclic pressuremeter with multiple cells for evaluation of liquefaction resistance of soils, ISP5, 2005
- [15] Reiffsteck P., Saussaye L., Habert J., Borehole quality influence on expansion test results, this conference
- [16] Briaud J.L., The Pressuremeter, A. A. Balkema, Rotterdam, Netherlands. 1992
- [17] Benoît J., Reiffsteck P., Getchell A., In situ empirical determination of earth pressures at-rest, this conference
- [18] Ishihara, K. Liquefaction and flow failure during earthquakes. Géotechnique 1993, 43, No. 4: 349-415.
- [19] Robertson, P. K. Interpretation of cone penetration test: A unified approach, Canadian Geotechnical Journal, 46 (1), 2009, pp. 1337-1355
- [20] Youd, T.L., and I.M. Idriss. "Liquefaction resistance of soils: Summary report from the 1996 NCEER and 1998 NCEER/NSF Workshops on Evaluation of Liquefaction Resistance of Soils." J. Geotech. Geoenviron. Eng. 127(10), 2001: 817-833.